Seismic surveys at the Per Geijer iron oxide-apatite mineralization in Kiruna, Sweden

Niklas Juhojuntti[1] and Łukasz Sito[2]

5 [1]Luossavaara-Kiiirunavaara AB, Sweden
[2]Geopartner Geofizyka, Poland

Correspondence to: Niklas Juhojuntti (niklas.juhojuntti@lkab.com)

10 **Abstract.** LKAB currently runs an intense exploration program focused on the Per Geijer (PG) iron oxide-apatite mineralization, close to the active Kiruna mine, in northern Sweden. The mineralization and the hosting volcanic units dip at an angle of 50-60 degrees and are overlain by quartzite. Greenstones are also present in the area. The iron mineralization is associated with high levels of phosphorus and REEs. As a major part of the mineralization occurs at depths >500 m, various geophysical surveys have been used to assist the exploration throughout the years, recently also including seismic
15 measurements. An initial pilot reflection profile in 2021 showed promising results, and three additional profiles were acquired shortly afterwards, all with Vibroseis as a source. These were followed by downhole seismics (VSP) in two drill holes. During 2024 a 3D survey covering the Per Geijer mineralization was also acquired. Clear P-wave reflections are visible in the shot records from the surface seismics as well as in the downhole seismics, and the latter also show interpreted P-S reflections. The steeply dipping structures in the area complicate the data processing, and out-of-the-plane reflections are
20 present in some of the 2D profiles, the latter confirmed via cross-dip analysis. The resulting migrated sections and volumes show prominent reflections, some of which correlate with the Per Geijer mineralization or units close to it and suggest some extensions of the known mineralization. Reflections are also observed from the northern end of the nearby Kiirunavaara ore. Sonic and density logs are available to support the interpretation. These indicate that the main cause of the reflections from the iron mineralization is the density contrast, rather than the velocity contrasts. The downhole seismics also allow a closer
25 link to the drilling information. Further notable in both our 2D and 3D surface data is a high-amplitude reflection originating from a steeply dipping structure outside the survey area, which if projected to the surface correlates with older greenstones on the western side of the Kiirunavaara orebody.

1 Introduction

Seismic reflection measurements are nowadays used by the mining industry both for exploration purposes and to assist the
30 planning of mine infrastructure (e.g. Malehmir and Bellefleur, 2009; Juhojuntti et al.; 2012; Donoso et al., 2022; Hloušek et al., 2025). For deep targets, it can potentially provide higher spatial resolution than any other geophysical method. There is ambiguity in the interpretation, as the reflections can be caused by various subsurface structures, for example deformation

zones or lithological contacts. For generating mineral exploration targets the method is probably best used in combination with other techniques, such as magnetotellurics. The typical mineral exploration setting can often have steeply dipping

35 structures, which pose a challenge for seismic imaging.

During the recent years there has been much exploration drilling and geophysical measurements towards the Per Geijer iron oxide-apatite mineralization, located close to the Kiruna mine, where the Kiirunavaara orebody is being mined via subsurface caving (Malmgren et al., 2007). The Per Geijer mineralization and the hosting volcanic units dip at an angle of 50-60 degrees and are overlain by quartzite. The iron mineralization is associated with high levels of phosphorus and REEs.

40 As a major part of the mineralization occurs at depths >500 m, various geophysical surveys have been used to assist the exploration throughout the years, recently also including seismic measurements. An earlier reflection survey did show a reflection interpreted to originate from the Kiirunavaara orebody (Jensen et al., 2012), which has a similar dip as the Per Geijer mineralization, although the host rock environment differs somewhat. Pronounced seismic reflections have also been observed in connection with the Blötberget iron mineralization in central Sweden (Pertuz et al., 2021; Hloušek et al., 2022).

45 The purpose of the seismic surveys at the Per Geijer field were to image the iron mineralization, detect possible unknown mineralization in the vicinity, and to map deformation structures. The survey program was initiated by a pilot reflection profile in 2021, to test the potential of the method in the Per Geijer area. As this profile showed promising results, three additional profiles were acquired shortly afterwards, using a larger number of more densely spaced receivers. We then carried out downhole seismics (VSP) in two drill holes. In connection with the VSP survey a small 3D grid was deployed on

50 the surface. As this small 3D survey showed promising results, a larger 3D survey was subsequently carried out. All these data have been acquired with Vibroseis as the seismic source, except for an accelerated wight-drop source being used for some sensitive parts of the 3D survey area.

We outline the processing of the seismic data and describe the observed reflections. The seismic images are compared with available geological models, making the case that the iron-oxides in the area are causing pronounced reflections and thus that

55 the seismic reflection method can be an effective exploration tool for such deposits. We also attempt to explain the physical cause of the reflections, using sonic and density logs.

2 The iron ores in the Kiruna area

The Kiirunavaara iron oxide-apatite (IOA) orebody is the type example of the IOA mineralisations (REF). It has been mined continuously since the year 1902, and the current main haulage level is 1365 meters below the former top of the mountain.

60 Much has been written about the geological setting and origin of this orebody (Geijer, 1910). There are several other IOA mineralisations in the immediate surroundings, many of which have been mined at least partially. The Luossavaara orebody, which was mined until the early 1980s is located just north of Kiirunavaara. East of the Luossavaara orebody there are several small mineralisations (Rektorn, Haukivaara, Henry and Nukutus) collectively called the Per Geijer ores that were also mined as open pits in the early to mid-20th century. In the 1960's a long-wavelength magnetic anomaly just north of

Kiruna town led to the discovery of the Per Geijer Deep mineralisation (PG Deep), which is the down-dip expression of the surficial Per Geijer mineralisations and the main target for the seismic surveys discussed in this article.

The Kiirunavaara, Luossavaara and PG Deep IOA deposits are all roughly disc-shaped bodies, striking approximately north-south and dipping 50-60 degrees to the east (Figs. 1 and 2). The Kiirunavaara orebody is about 4 km long and on average 80 m thick, increasing to about 200 m in the north. The iron oxides in Kiirunavaara and Luossavaara are almost exclusively magnetite, whereas the PG Deep mineralization is a mix of magnetite and hematite. PG Deep is associated with significant amounts of phosphorus and REE's (LKAB, 2024).
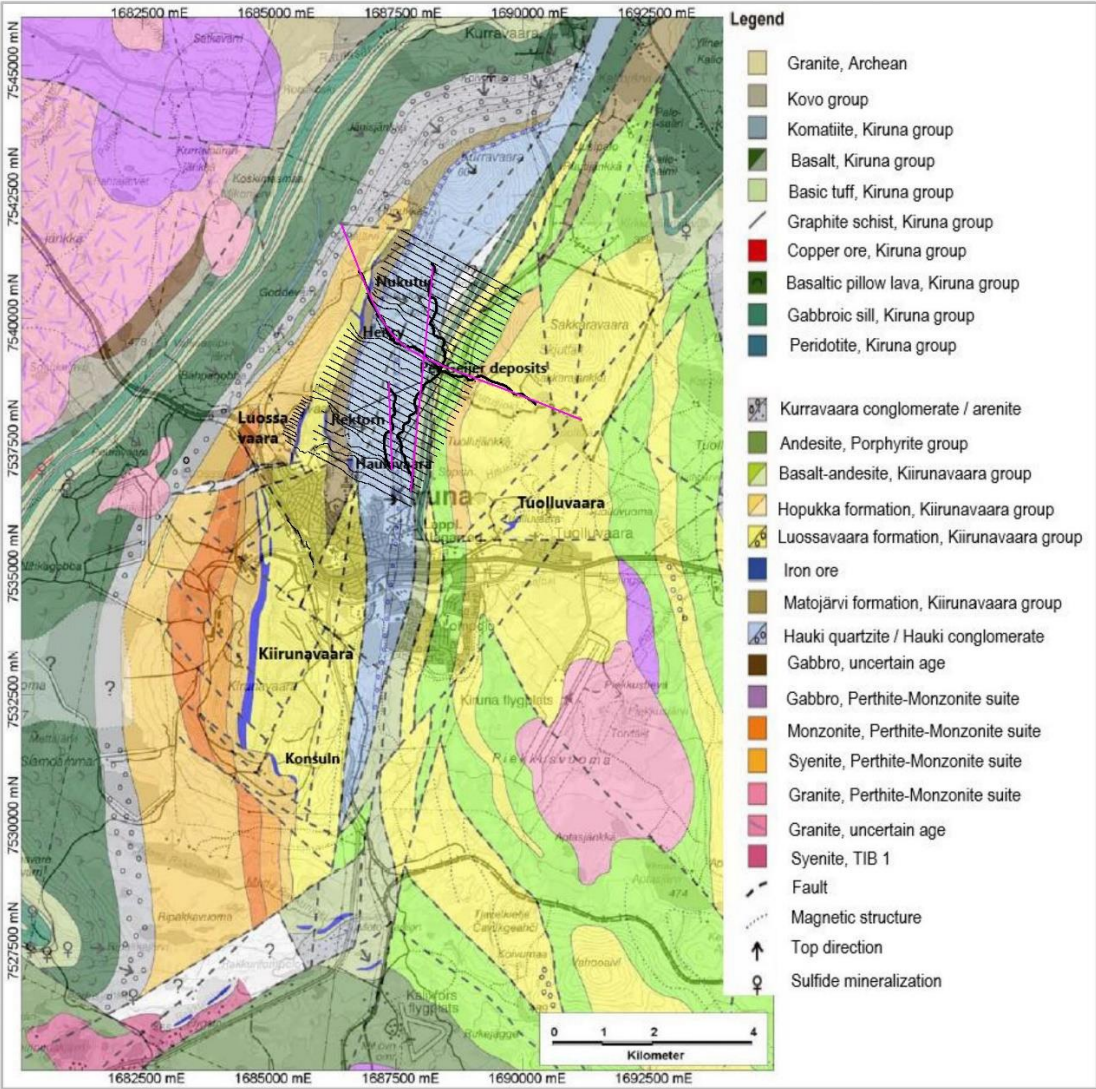
Figure 1: Geology of the Kiruna area and the location of the seismic surveys. Only the seismic receiver points are shown, not the source positions for the 3D survey. The CDP projection lines for the 2D profiles are also shown, in purple. Geological map modified from Martinsson and Erlandsson (2009).

The Kiruna area is divided in two major volcanosedimentary belts with different ages that show a younging direction from west to east, dipping approximately 50–60 degrees (Fig. 1). In the west the bedrock consists of the early Paleoproterozoic Kiruna greenstone belt, which mainly comprises mafic volcanic rocks, gabbroic units and graphite schist. The Kiruna

80 greenstone belt is clearly visible in gravity and electromagnetic surveys. The overlying Kurravaara conglomerate unit separates the younger Kiirunavaara group from the greenstones. The IOA deposits in the Kiruna area are located within the volcanic and volcano-sedimentary formations of the Kiirunavaara Group (Fig. 1). The Kiirunavaara group starts with the trachyandesitic Hopukka Formation that forms the footwall of the Kiirunavaara and Luossavaara orebodies. The hanging wall consists of the rhyolitic-rhyodacitic Luossavaara Formation. The PG mineralisations are located between the volcanic

85 Luossavaara Formation and the overlying volcano-sedimentary Matojärvi Formation. Mineralisation can also occur exclusively within the Luossavaara Formation or in the Matojärvi Formation. The Matojärvi Formation is a complex volcano-sedimentary pile that hosts hematite-dominant and mixed hematite-magnetite mineralisation which are commonly seen to replace the host lithologies. It is covered by a slightly metamorphosed, thick, sedimentary basin-derived package (quartzites, conglomerates and phyllites of the Hauki Formation). The Hauki Formation has very low magnetization and

90 electrical conductivity.
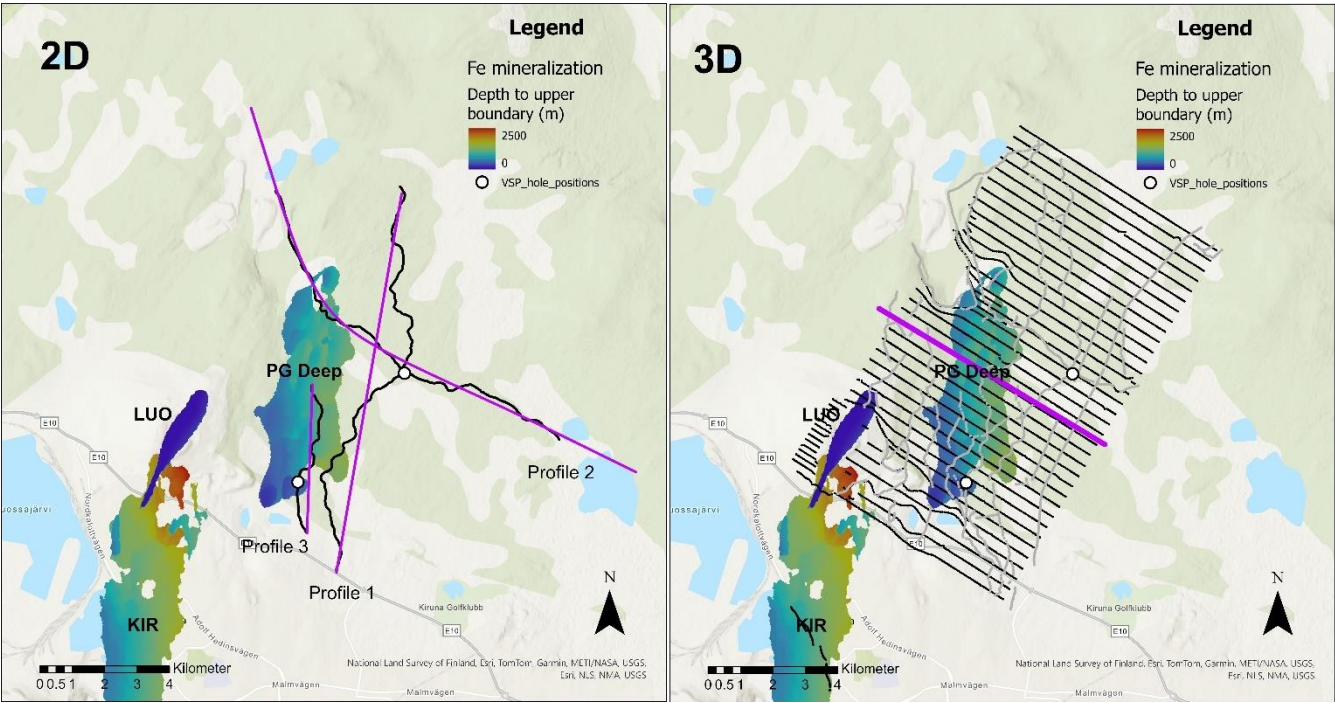
Figure 2: The seismic surveys in comparison with the iron-oxide deposits in the Kiruna area, colored by the depth to the upper boundary: KIR – Kiirunavaara, LUO – Luossavaara, PG Deep – Per Geijer Deep. Black symbols show receivers and grey symbols source points. For the 2D surveys, the source points overlap with the receivers. The purple symbols show CDP projection lines and
95 **the inline selected for display in Fig. 8. The two VSP holes are also shown. Background map credits: National Land Survey of Finland, Esri, TomTom, Garmin, METI/NASA, USGS, NLS, NMA.**

3: Physical rock properties

Sonic and density logging have been carried out in some of the exploration holes in the Per Geijer area, and one example is shown in Fig. 3. There is a distinct density increase in the Fe mineralization, as expected. The Matojärvi formation overlying

100 the mineralization also has intervals with high density. The quartzite and porphyry intervals have markedly lower densities. The P-wave velocity was difficult to measure in the shallow part of the hole. However, it appears to be around 4 km/s in the quartzite unit, increasing to about 5.5 km/s in the porphyry. At the onset of the Matojärvi formation, at about 300 m, the velocity increases to around 6 km/s. It is difficult to see any distinct change in the P-wave velocity associated with the iron-oxide mineralization, although there is an interval with somewhat higher velocity around 450 meters depth, within the

105 mineralization. It was difficult to measure reliable S-wave velocities in this drill hole, and these are not shown here. However, where it was possible to measure with some degree of accuracy, the Vp to Vs ratio is around 1.8. Note that this drill hole is dominated by hematite. For comparison, Malmgren et al (2007) report P-wave velocities in the range 5.8-6.2 km/s for undisturbed magnetite iron ore in the Kiruna mine. Measurements on magnetite core samples from the Kiruna area show average P-wave velocities of around 6.2 km/s, although individual samples show considerable spread around this

110 value.
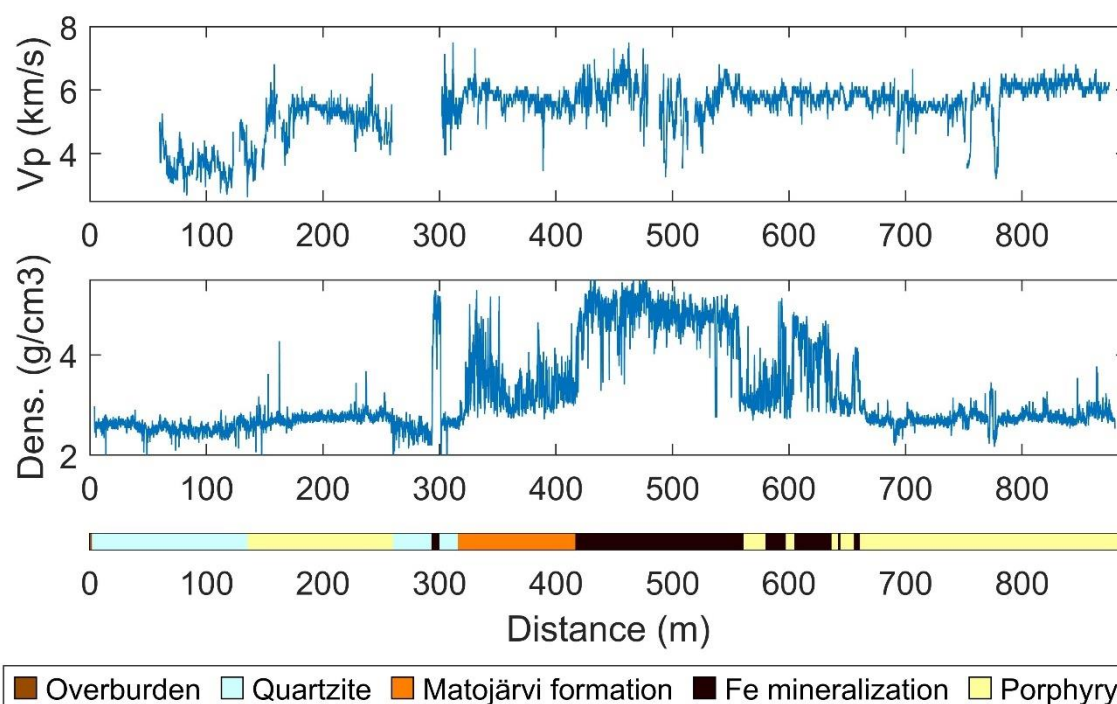
Figure 3: Wireline logs from one drill hole intersecting the Per Geijer Deep iron mineralization. The lithology description has been somewhat simplified.

4 Seismic surveys in the Per Geijer area

4.1 Surface and downhole seismic data acquisition

Seismic data have been recorded along three 2D profiles, and in one 3D survey covering most of the survey area (Fig. 2). Downhole seismic (walkaway VSP) data were also acquired in two drill holes. While running the downhole surveys, a small 3D receiver grid was deployed at the surface, recording the signals used for the downhole seismics. This smaller 3D survey is not included in this paper, although it was a catalyst for proceeding with the larger 3D survey.

The same Mark IV Vibroseis source have been used for all seismic surveys, including the walkaway-VSP. For the 3D survey we also used an accelerated weight-drop source in some sensitive areas, although these data have been processed separately and are not included in this study. The signal strength of the weight-drop source was significantly lower than for the Vibroseis truck.

It was necessary to use existing trails and roads for the Vibroseis truck (and the accelerated weight-drop), which was a particularly limiting factor for the 2D surveys. The north-south oriented Profile 1 and 3 are almost parallel to geologic strike, which is not ideal for interpreting the data. For the 2D surveys a combination of WiNG and GS-One 10 Hz sensors were used, and the station spacing varied between 5 and 10 m. Profile 2 was acquired in two campaigns with some station overlap and different recording parameters, which is reflected in the variable fold.

The 3D survey was acquired with a regular grid of approximately east-west oriented receiver lines, with inline receiver spacing of 20 m and crossline receiver spacing of 140 m. Stryde sensors were used for this grid. The source lines were oriented roughly perpendicular to the receiver lines. Difficult terrain access prevented us from extending the 3D survey further to the east, which could have allowed better imaging of the PG Deep mineralization. During the 3D survey the Vibroseis force was reduced to 50 % (from the nominal 75 %) along some roads. A small receiver layout of WiNG nodes was also placed close to the Kiruna mine (Fig. 2), to investigate the noise conditions in this area and to possibly observe wide-angle reflections from mineralization between Per Geijer and Kiirunavaara using the 3D survey source points. These data were rather noisy and are not discussed further in the paper, although it is possible to detect P-wave energy in many of the shot records.

Walkaway VSP measurements were carried out for two holes (Fig. 2). The data were acquired using fiberoptic cables and the same Vibroseis truck as used for the surface measurements. The source points were located along the same roads as used for Profiles 1 and 2 (Fig. 2). It was not possible to cement the fiberoptic cables in place. However, as both holes were waterfilled the coupling should have been adequate. We here focus on the survey from the northern hole, as the data from the southern hole were more noisy, possibly due to water flow from a fracture zone crossing the hole. The fiberoptic cables were straight and therefore only sensed axial motion.

4.2 Surface seismics data processing and analysis

145   Reflections can be observed in many of the shot records (see example data in Fig. 4). Note for example the prominent reflection at about 0.2-0.3 s. There is also a reflection at roughly 1.0-1.5 s, apparently from some steeply dipping structure. Some shot records also show a prominent reflection at about 2 s, apparently also from some dipping structure.

Conventional algorithms have mainly been used for the data processing, as summarized in Table A1 in the Appendix. Similar processing sequences have been applied for all the 2D profiles, followed by post-stack migration and depth-

150   conversion to generate the seismic images. For the 3D dataset, two different processing approaches were used, one based on pre-stack time migration and wider bandwidth, and the other based on post-stack migration and lower frequencies. The first approach was focused on imaging the main target of the survey, the Per Geijer Deep mineralization, with as high resolution as possible. The second 3D processing approach was aimed at imaging deeper targets using lower resolution, while also having a more simplified processing flow less likely to generate artefacts. CPU limitations put constraints on the maximum

155   size of the image volumes for the pre-stack migration.
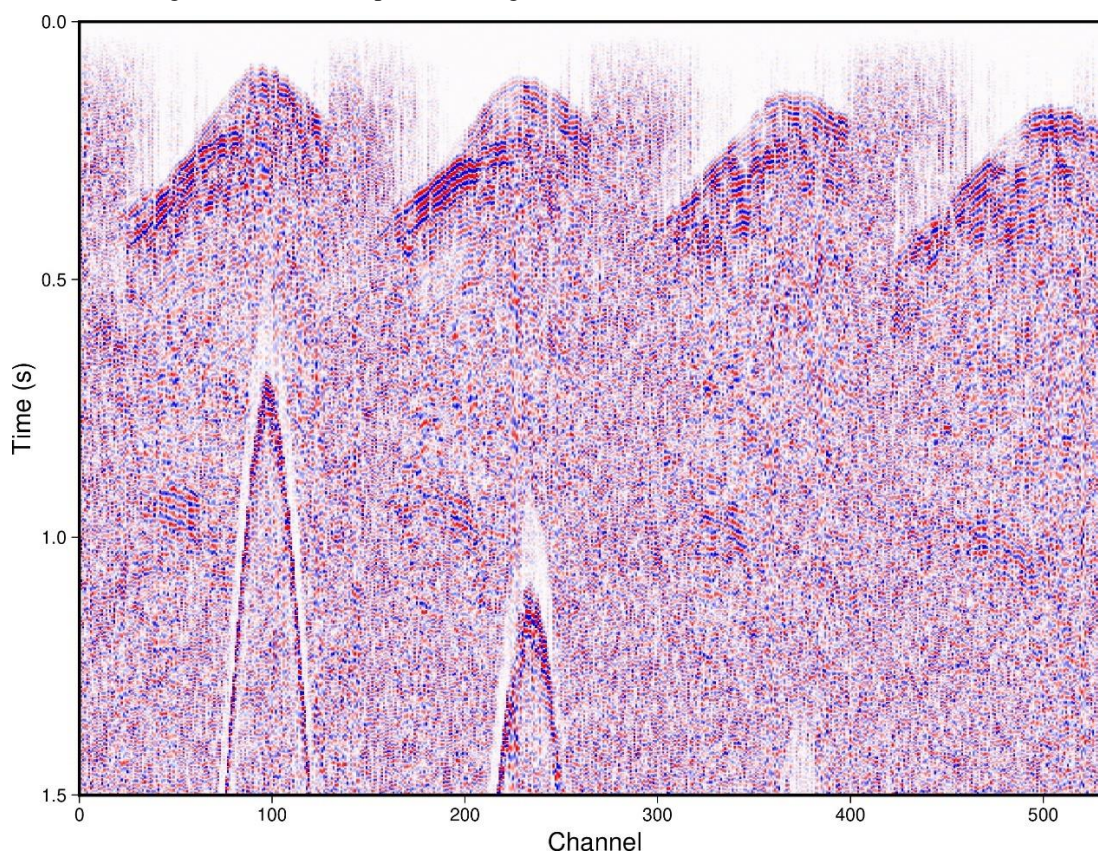
Figure 4: Example shot record data, from the 3D survey. The image only shows a subset of channels. Automatic gain control and some frequency filtering has been applied prior to plotting.

160   Overall, the seismic data show pronounced static shifts, as evident from the first arrivals and the reflections. Refraction static corrections have therefore been an integral part of the processing flow. For all datasets, the refraction statics have been calculated based on velocity models with two layers, the first representing the overburden with a fixed velocity, the second layer representing the bedrock with smooth velocity variations allowed. Residual reflection statics were also used to further remove short-wavelength static shifts. All surface seismic data have been processed to a fixed datum of +450 m relative to

165   sea-level.

Surface-consistent deconvolution (Cary and Lorentz, 1993) was used for the 3D data input to pre-stack time migration, mostly to improve waveform consistency, although it will also compress the waveform to some degree. For the 2D profiles, spectral equalization was used instead. These spectral adjustments were followed by time-varying bandpass filters, with gradually decreasing filter frequencies towards later times to account for the loss of high frequencies due to attenuation. For

170   the second 3D processing approach including post-stack migration and aimed at deeper structures, no spectral adjustments or time-varying filters were used.
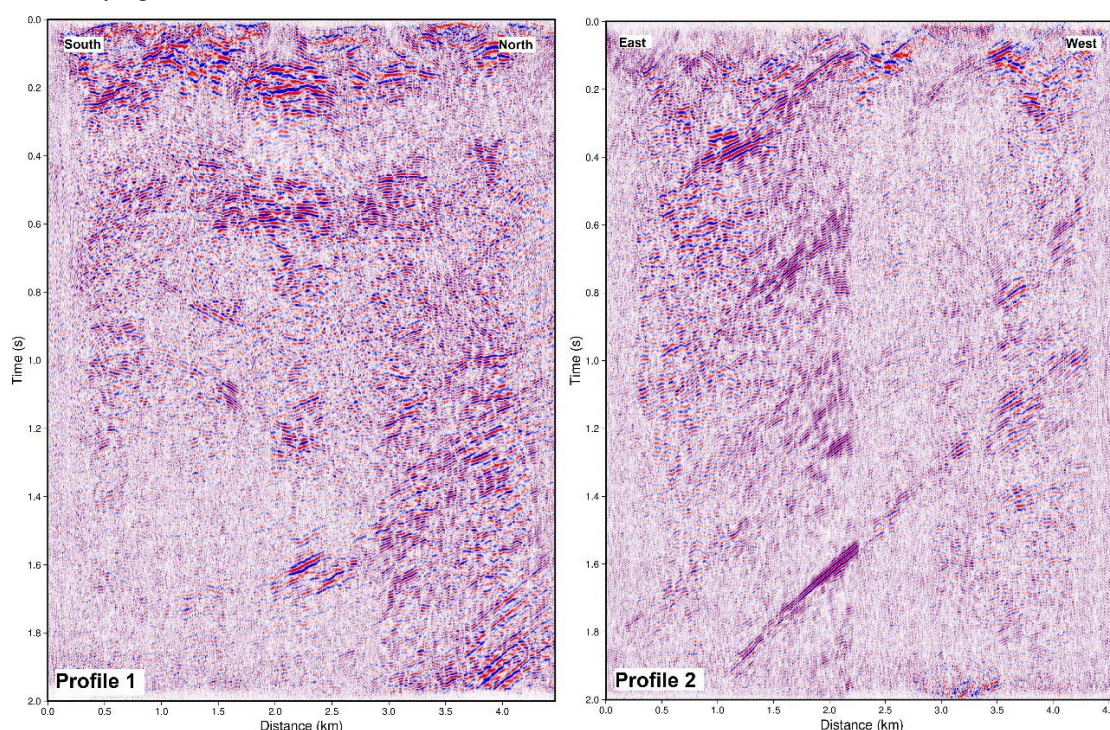
Figure 5: Stacked time sections from Profiles 1 and 2, unmigrated.

For the 2D profiles CDP stacking followed by post-stack migration was used, although it was challenging to find the proper

175   NMO velocity functions. Many of the reflections come from steeply dipping structures, and to stack these properly very high NMO velocities would need to be used, which is not optimal for the reflections from moderately dipping structures. The chosen stacking velocities were a compromise, higher than required for sub-horizontal reflections, while not as high as

would have been optimal for the steeply dipping events. Dip-moveout correction was tested but deemed not to give satisfactory results.

180 The stacked time sections from the 2D profiles show pronounced reflections, which in general are steeply dipping along Profile 2, and appear more moderately dipping or sub-horizontal along Profiles 1 and 3 (Fig. 5). The less pronounced apparent dip along the two latter profiles is mainly due to these profiles being oriented parallel to geologic strike. Note for example the gently dipping or sub-horizontal band of reflections at about 0.2 and 0.5 s along Profile 1 (Fig. 5). Diffractions are also visible at the northern end of Profile 1. However, the reflections along Profiles 1 and 3 are probably largely coming

185 from out of the plane, given that most structures in the area are dipping to the east. Note that the fold is varying much along Profile 2, which is clearly noticeable in the stacked time section (Fig. 5).

To access the direction of the incoming seismic reflections, cross-dip analysis was carried out following the procedure of Wu et al. (1995). This method makes use of the crooked recording lines and is in a strict sense only valid for zero-offset reflections. It should nevertheless give indications of possible out-of-the-plane reflectivity also when there is considerable

190 shot-receiver separation, as for these data. The method involves choosing a set of cross-dip angles (including zero), calculating pre-stack time shifts for these, and visually observing which of these angles maximizes the amplitude of a particular reflection in the stacked section. The example shown for Profile 3 indicates that much of the reflected energy is coming from structures dipping to the east and located to the west of profile (Fig. 6). The reflections denoted R1 and R3 have higher amplitude and appear most coherent when using a cross-dip of 30 degrees to the east. However, reflection R2

195 seems to come from a structure with little cross-dip. None of the reflections become more coherent when using a cross-dip towards west.

Profile 2 is oriented more favorably for correctly imaging the dip of the reflections, and the migrated depth section shows several east-dipping reflections (Fig. 7). The reflection at about distance 4 km along the profile, and at a depth 1.5 km, coincides with the Per Geijer Deep mineralization.

200
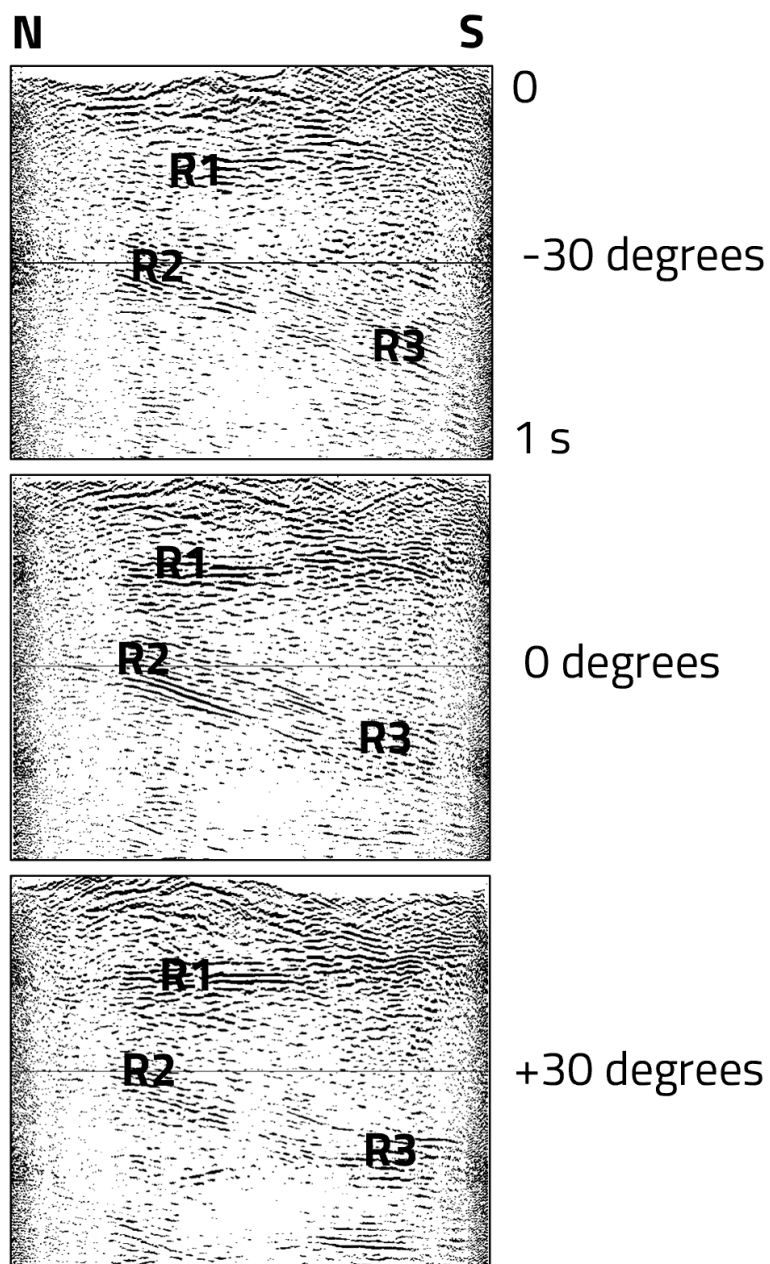
Figure 6: Cross-dip analysis for Profile 3. The dip is defined as positive towards east.

205
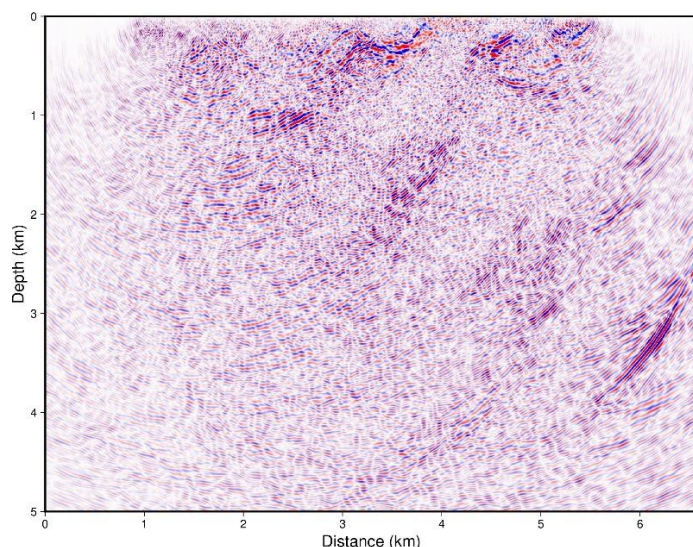
Figure 7: Depth section from Profile 2, post-stack migrated. The profile has been padded by 1 km at both ends.

The 3D survey should be able to handle reflections with different dip directions in a better manner than the 2D profiles. However, the issue with the difficulty of simultaneously stacking moderately and steeply dipping reflections remains, when

210 using CDP stacking followed by post-stack migration. The steeply dipping reflections will also cause reflection point dispersal or smearing. Pre-stack migration have therefore been used to handle variations in the dip of the reflectors. The velocity variations in the area are considered moderate, and therefore pre-stack time migration was judged to give sufficient accuracy. An example of a pre-stack migrated depth section is shown in Fig. 8 (see Fig. 2 for location). A steeply east-dipping reflection is observed, at the location of the main survey target, the Per Geijer Deep mineralization.

215 Further to this, a second approach have been used for the 3D processing, based on post-stack migration and lower frequencies, results of which are shown later in the paper. In this case, the chosen NMO velocities were moderately high.

All surface seismic data have been depth-converted using a constant velocity of 6000 m/s.

4.3 Downhole seismic data processing and migration

Example walkaway VSP data from the approximately 1700 m long northern hole are shown in Fig. 9. The down-going P

220 wave is generally seen throughout the entire hole. The uniaxial response of the fiberoptic cable could explain the apparent decrease of the P wave amplitude along some intervals of the hole, for which this seismic wave would arrive from the side of the hole. One of the records in Fig. 9 also show signs of down-going S-wave energy.
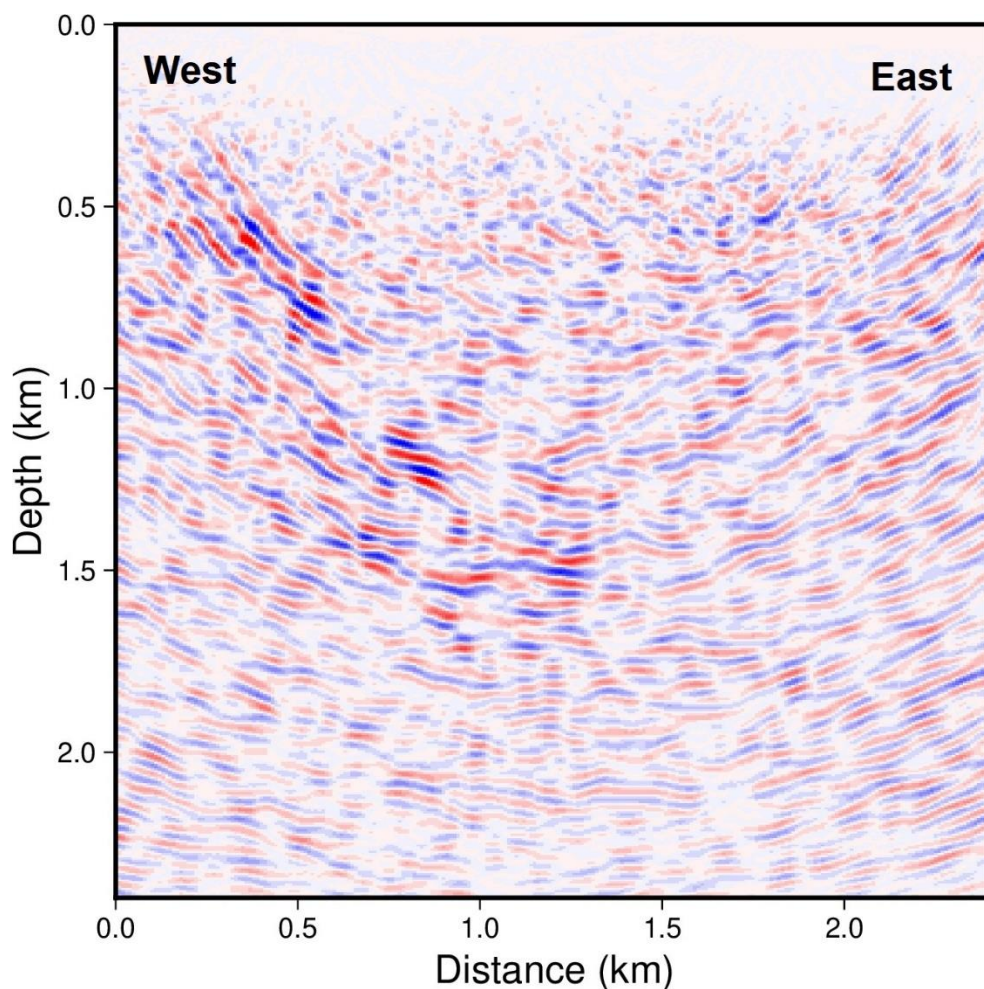
Figure 8: Example inline from migrated 3D depth volume.

Upgoing waves interpreted to be P-wave reflections (PP) can also be observed, originating from about 1500 m distance along the drill hole. The Fe mineralization in this hole is mainly occurring within the intervals 1450-1550 m and 1650-1700 meters. There are signs of P-S converted reflections in some records, more clearly seen for source points at some distance from the drill hole.

To enhance the reflected waves prior to migration, median filtering was used to suppress the down going P and S waves, and the strong tube waves. Source statics from the simultaneous small surface 3D survey were also applied to the downhole seismic data.

For the migration, a basic migration code able to handle the downhole geometry was implemented. It assumes constant velocities and projects the amplitude for each data point onto an ellipsoid in the 3D volume surrounding the drill holes and
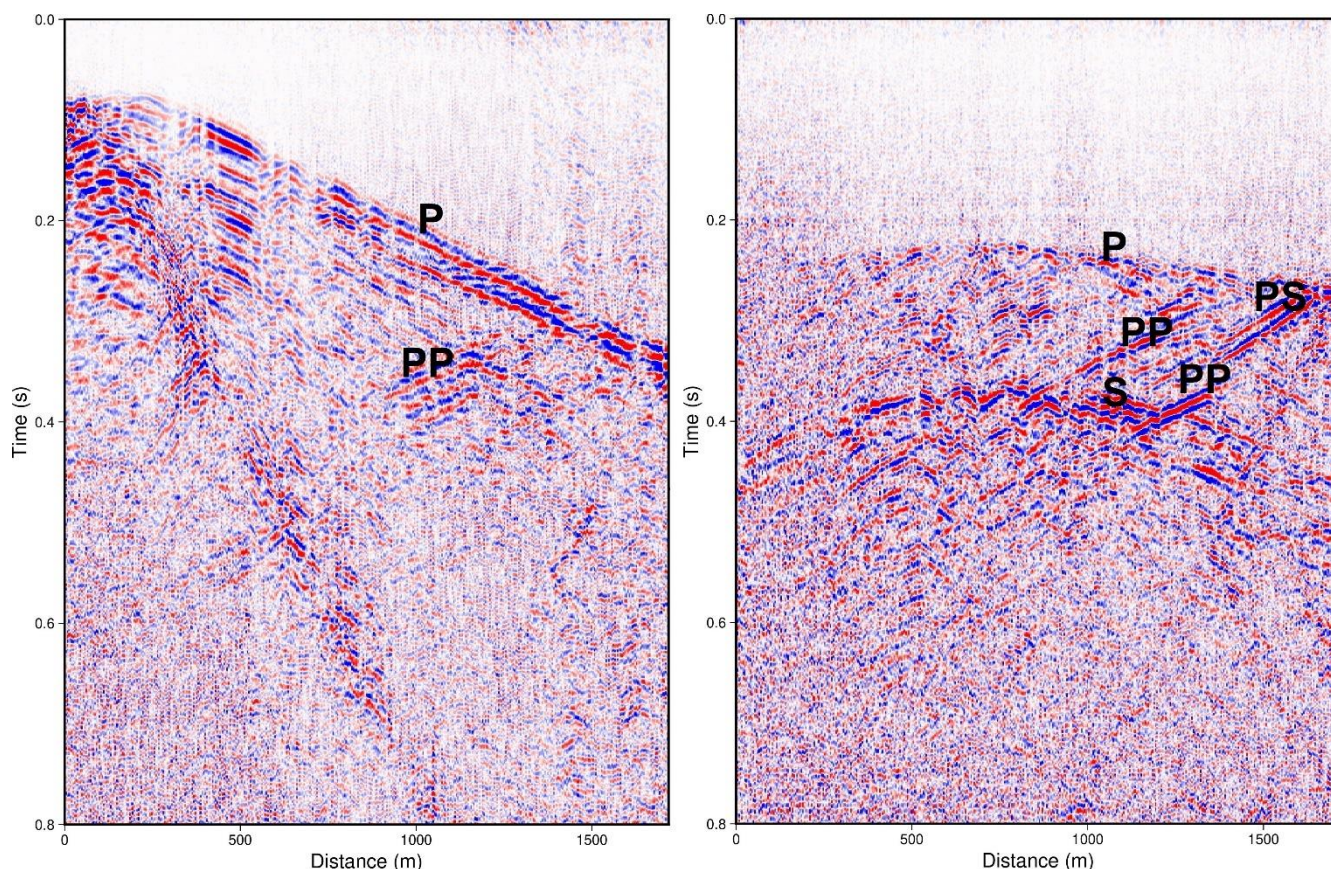
Figure 9: Example data from the walkaway VSP survey. Increasing depth towards right. For the record to the left the source point is close to the drill hole, for the one to the right the source is further away. For clarity, the tube waves have been suppressed prior to display. Spectral balancing and AGC have also been applied. See text for description of the annotated seismic phases.

the source point, taking the proper recording geometry into account. These ellipsoids are then summed to produce the migrated image. No amplitude corrections are included in the summation process, and the uniaxial response of the fiberoptic cable has not been accounted for. A selection of Vibroseis source points close to the drill hole were included in the migration, those further away were not used. The resulting migrated image shows a prominent reflection in good agreement with the model of the Fe mineralization (Fig. 10). A velocity of 5000 m/s was chosen for the migration, and the inherent depth conversion.

245
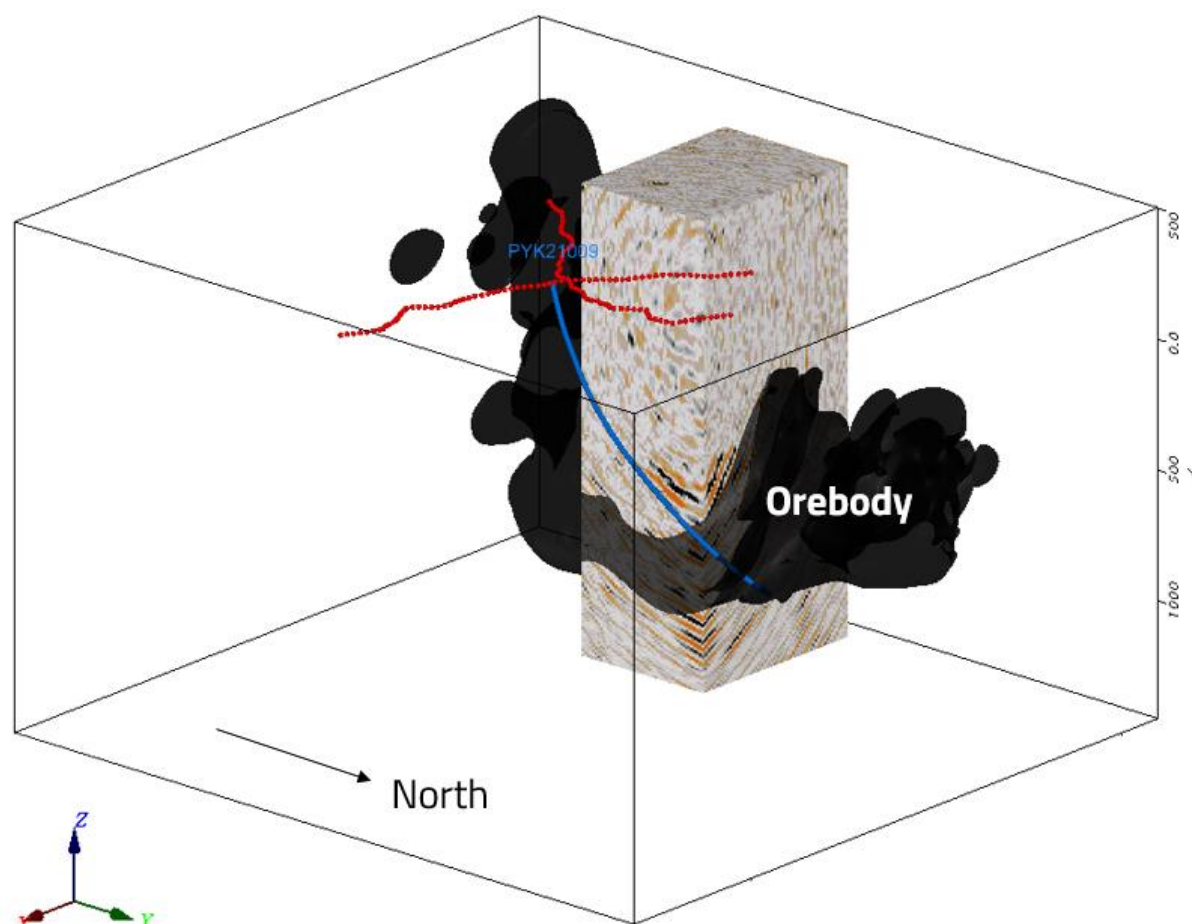
Figure 10: Migrated depth volume from the walkaway VSP survey. The drill hole is shown in blue, and the red dots represent the source positions used for the migration.

5 Integration and interpretation

The Kiirunavaara and Per Geijer iron-oxide deposits are well-constrained by drilling, and there are recently updated

250 geological models for comparing with the seismic results. Various non-seismic geophysical surveys have also been conducted in the area, including geophysical wireline logging in many holes.

A comparison between the pre-stack migrated 3D seismic image and the deposit model for Per Geijer Deep shows a clear correlation between the most distinct reflections and the iron-oxide volume (Fig. 11). This is observed in all the seismic data from the Per Geijer area, and particularly evident in the migrated image from the walkaway-VSP survey (Fig. 10). Although

255 it is often difficult to tie the reflections directly to the contacts of the iron mineralization, it seems likely that these iron-oxide deposits are causing much of the associated seismic reflectivity.
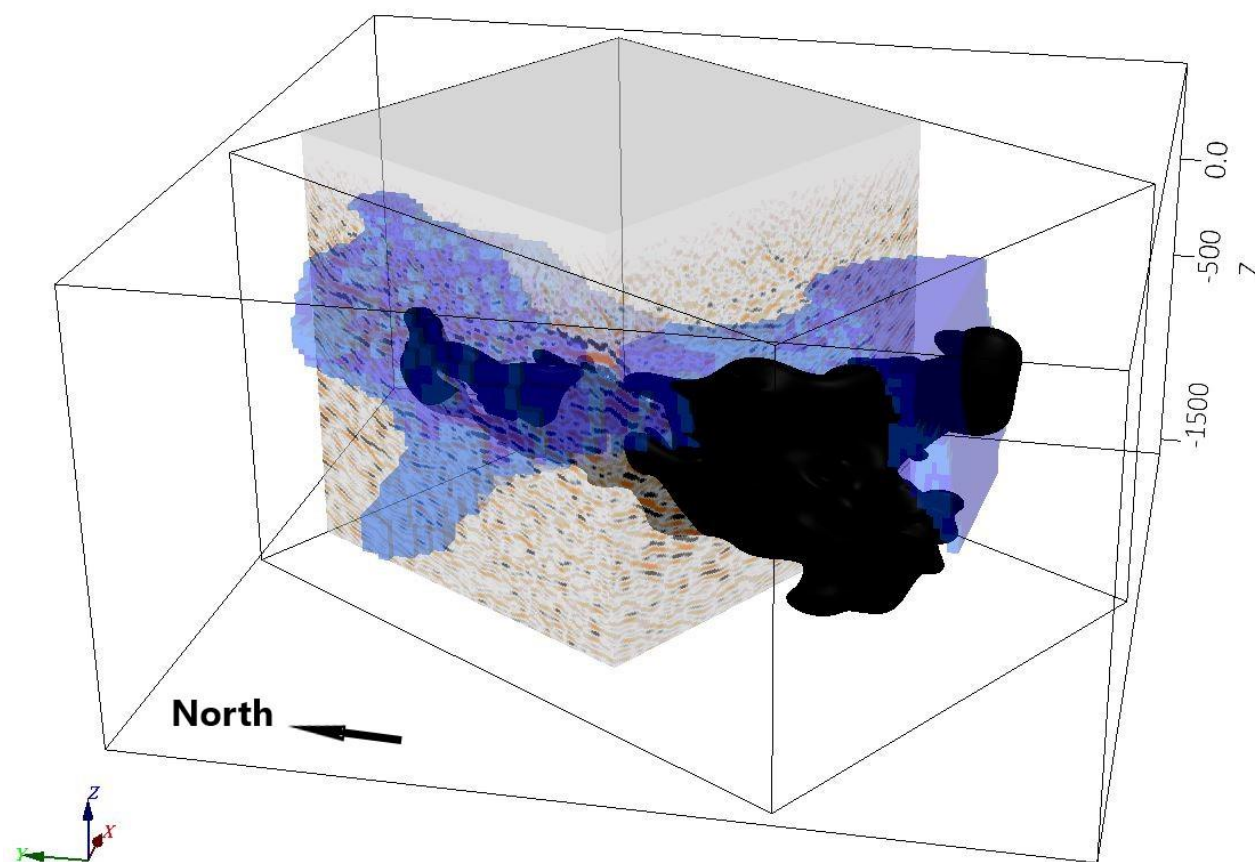
Figure 11: Pre-stack migrated depth volume from the 3D survey, in comparison with the geological model for the Per Geijer Deep mineralization, shown in black. Also shown in blue is the electrical conductivity model from a semi-airborne EM survey (Smirnova et al, 2020). All cells with conductivity >0.02 S/m are shown. The seismic volume and the conductivity model are semi-transparent.

Profiles 1 and 3 are oriented roughly parallel to the strike of the mineralization and most lithological contacts in the area, and therefore it would not be likely to see a correlation between the seismics and the geological models if the seismic sections were plotted vertically. Instead, we compare the seismic sections with the geological models after tilting the sections towards west, in the expected direction of the incoming reflections, an example of which is shown for Profile 3 in Fig. 12. There is a clear correlation between the reflections and the occurrence of iron-oxides.

Although the 3D survey was designed to image the Per Geijer Deep mineralization, reflections are also observed from the northern end of the nearby Kiirunavaara iron-ore. This is clearly seen in the 3D seismic image from the post-stack migration processing sequence (Fig. 13B). An earlier seismic profile in the area also showed a reflection interpreted to originate from the Kiirunavaara ore (Jensen et al., 2012).

The sonic log in Fig. 3 only shows a slight increase in the P wave velocity for the Per Geijer Deep mineralization, and the S wave velocities show an even less distinct change. Therefore, velocity variations do not appear to be the main cause of the observed reflections. However, the density contrast between the iron-oxides and the host rock is significant. To quantify the
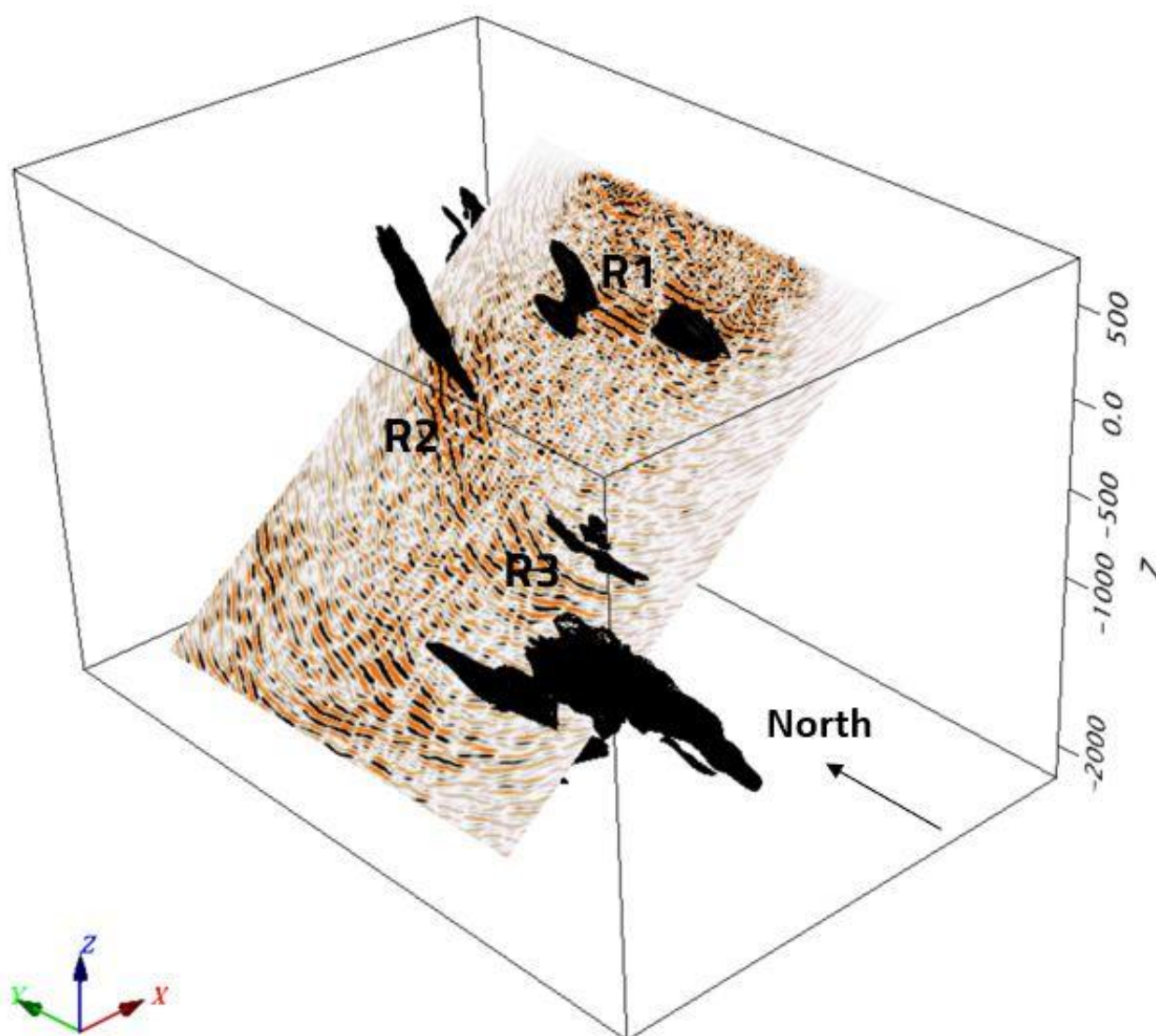
Figure 12: Depth section from Profile 3, plotted at an angle to account for the reflections mostly coming from the western side of the seismic line. The geological models for the iron-oxides are shown in black.

reflectivity of the iron-oxides, reflection coefficients for P-P and P-SV reflections have been calculated. Approximate equations which assume small contrast in elastic properties were considered sufficient for this case (see p. 256 in Kennett, 2001). Based on the logs in Fig. 3, a P-wave velocity increase from 5.5 to 6.0 km/s and a density increase from 3.0 to 4.4 g/cm^3 were assumed to reasonably represent the contact of the mineralization. Lacking better information, the S-wave velocities were assumed to follow the P-wave velocities via the normally assumed ratio of 1.72 between these two. The calculated P-P reflection coefficient is approximately 0.28 at vertical incidence, decreasing to about 0.08 at an incidence of 55 degrees (Fig. 14). At larger incidence angles the approximate equations fail, and such angles should in any case be
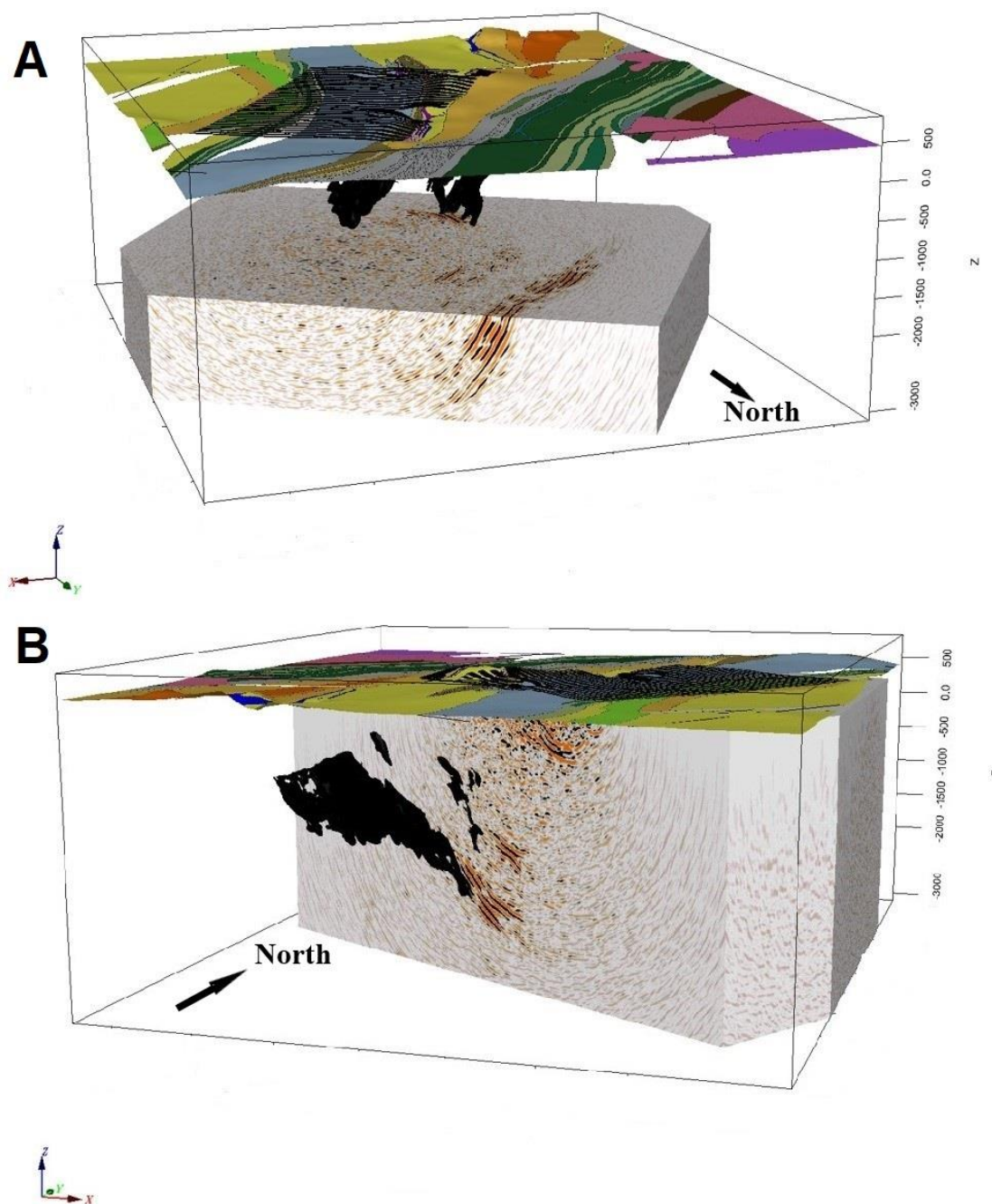
Figure 13: Post-stack migrated depth volume, showing deep reflections. The geological models are shown for comparison. The large unit is the northern end of the Kiirunavaara ore. Note that in image A the upper boundary of the seismic cube is at elevation -1700 m. The geological map from Fig. 1 has been draped on the surface, and the 3D receiver is also shown.

uncommon for our survey geometries. The reflection coefficient only decreases slightly if no velocity contrasts are assumed, and the amplitude trend with respect to the incidence angle does not change significantly. It should though be noted that the

Matojärvi formation close to the PG Deep mineralization also can contain relatively dense mafic lithologies (Fig. 3), potentially generating reflections.

Of relevance to the walkaway VSP survey, the P-SV reflection coefficients were also calculated (Fig. 14), using the same
295 parameters as for the P-P reflection calculations. The P-SV reflection show zero amplitude at normal incidence, and an increase in amplitude with incidence angle. This agrees with the P-SV being observed more clearly for source points further away from the drill hole (Fig. 9).
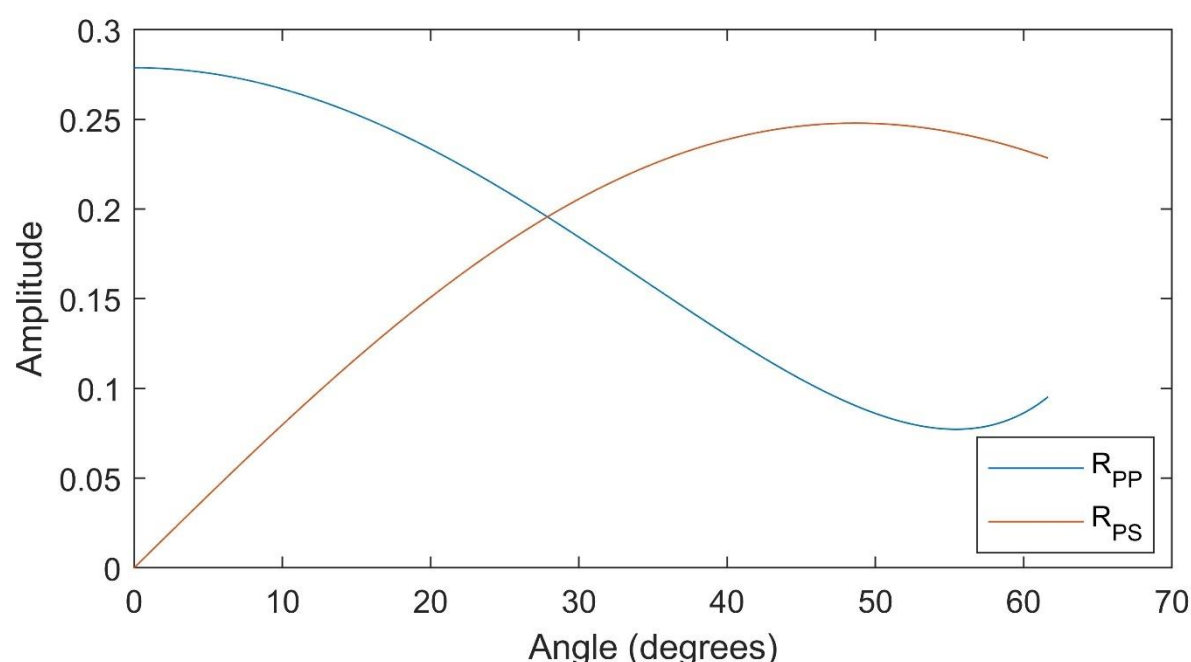
Figure 14: Calculated reflection coefficients for the Per Geijer Deep mineralization. The angle is measured relative to vertical,
300 **with 0 degrees referring to normal incidence.**

The Luossajärvi mineralization (see Figs. 1 and 2 for location) does not have a clear expression in the 3D seismic data. The reflection R2 in the tilted depth section from Profile 3 (Fig. 12) correlate roughly with an extension of the mineralization towards depth. However, the cross-dip analysis indicated that this reflection originates underneath the profile and not to the west.

305 In some cases, the seismics indicate extensions to the mineralization models. One example is along Profile 2, where the migrated section shows the reflection at about 4.5 km along the profile extending to depths of about 2 km, which is deeper than reached by any drill holes in this area. This is however on the limit of the depth penetration of the survey, considering the steep dip of the mineralization.

An obvious question from an exploration perspective is whether there are signs of unknown mineralization in areas not
310 covered by the drilling. Discussing this in detail is not the scope of this paper. There is however a reflection at about 2 km along Profile 2 (Fig. 7), which roughly coincides with a deep EM conductor observed in the semi-airborne EM survey from

the DESMEX project (Smirnova et al., 2020). However, the reflection could also be associated with the greenstones present in this area (Fig. 1), which on their own are not exploration targets. As observed in Fig. 12 the Fe mineralization does generate a response in EM surveys, indicating that a combination of seismics and EM should be an effective exploration tool for these types of deep-seated deposits.

There are also at least two reflections to the west of the actual survey area, beyond the reach of any drill holes (Fig. 13A). The most pronounced one is also clearly seen in Profile 2 (Fig. 7), and it was a dominating feature in the small 3D survey mentioned earlier. A possible explanation could be the 2.40-1.96 Ga basalt-andesite units to the west of the survey area, judging by where the reflection projects to the surface. There are also graphite units to the west of the survey area, and ground and airborne EM shows a pronounced conductor in the area (Smirnova et al., 2020). Sparsely located dynamite shots during an earlier reflection seismic profile in this area indicated an east-dipping reflection, possibly extending to depths of 10 km or more (Juhojuntti et al., 2013).

The eastern part of Profile 2 crosses the regional Kiruna-Naimakka deformation zone (Bergman et al., 2001, Grigull et al. 2018, and references therein), although it is difficult to see any obvious expression of this deformation zone in the seismic data, possibly due to the steep dip. Comparisons have also been made between the seismics and the deformation zone mapping carried out in connection with the exploration drilling, discussing this is however beyond the scope of this paper.

6 Conclusions

Surface and downhole seismic reflection measurements have been carried out at the Per Geijer field, close to Kiruna. Distinct reflections are observed from the main target, the Per Geijer Deep iron-oxide mineralization, and from the nearby Kiirunavaara iron ore. The steep dips of most lithological boundaries in the area, including the contacts of the iron-oxides, pose a challenge for seismic imaging, both with respect to processing and data acquisition. Some of the seismic profiles were oriented almost parallel to the dominating strike direction in the area, which complicates the interpretation, although cross-dip analysis can be used to distinguish reflections coming from the side of the profiles. Downhole sonic and density logging indicates that the seismic response from the PG Deep mineralization is primarily caused by the distinct density contrasts. Pronounced reflections are also recorded from the footwall of the mineralization, possibly caused by mafic units.

Appendix

Table A1: Processing parameters.

2D processing	3D processing, pre-stack migration	3D processing, post-stack migration
	Vibroseis correlation and stacking	
	Geometry setup	
	Spherical divergence correction	
Bandpass filter: 10-20-150-220 Hz	Bandpass filter: 6-12-130-200 Hz	Bandpass filter: 7-14-50-80 Hz
Airwave mute	Airwave mute	Airwave mute
Spectral balancing, 10-20-140-180 Hz	Median filter, 2.5 km/s reject	Correction to fixed datum at 450 m
Median filter, 2.5 km/s reject	Surface-consistent deconvolution	Refraction static corrections
Bandpass filter, time-variant	Bandpass filter, time-variant	Automatic gain control, 500 ms
Automatic gain control, 300 ms	Front mute	Normal-moveout correction
Correction to fixed datum at 450 m	Correction to fixed datum at 450 m	Residual static corrections
Refraction static corrections	Refraction static corrections	Stack
Normal-moveout correction	Automatic gain control, 400 ms	Automatic gain control, 400 ms
Residual static corrections	Residual static corrections	FX Decon, 25 traces length
Stack	3D Kirchhoff time migration	Trace padding at sides
Automatic gain control, 400 ms	Time-to-depth conversion, 6 km/s	2.5D Stolt migration
FX Decon, 25 traces length		Time-to-depth conversion, 6 km/s
Trace padding at ends		
2.5D Stolt migration		
Time-to-depth conversion, 6 km/s		

340

Code availability

None of the computer codes used for the study are available.

Data availability

The data used for the study are not available.

Author contribution

Łukasz Sito have participated in planning the seismic surveys, organized much of the fieldwork, and prepared the Vibroseis data for further processing. Niklas Juhojuntti has carried out the further data processing and analysis, interpreted the data, and prepared the manuscript.

Competing interests

The authors declare no competing interests.

Acknowledgement

The company OptaSense deployed and operated the fiberoptic cable used for the VSP surveys, and GeoVista (Sweden) conducted the density logging. Laura Lauri from LKAB contributed to the geological description. Globe Claritas™ was used for the seismic data processing, except for the VSP migration which was coded in Matlab™. The Generic Mapping Tool (GMT) package and OasisMontaj™ were used to create most of the illustrations. The field crews of Geopartner and LKAB are thanked for their work during the seismic surveys.

References

Bergman, S., Kübler, L. and Martinsson, O.: Description of regional geological and geophysical maps of northern Norrbotten County (east of the Caledonian orogen), Sveriges geologiska undersökning Ba 56, 2001.

Cary, P.W., and Lorentz, G. A.: Four-component surface-consistent deconvolution, Geophysics 58, 383-392, 1993.

Donoso, G.A., Malehmir, A., Carvalho, J., and Araujo, V.: 3D reflection seismic imaging of volcanogenic massive sulphides at Neves-Corvo, Portugal, Geophysical Prospecting 71, 1116-1131, 2022.

Geijer, P.: Igneous rocks and iron ores of Kiirunavaara, Luossavaara and Tuolluvaara, Scientific and practical researches in Lapland arranged by Luossavaara–Kiirunavaara Aktiebolag, Stockholm, 278 pp, 1910.

Grigull, S., Berggren, R., Jönberger, J., Jönsson, C., Hellström, F.A., and Luth, S.: Folding observed in Palaeoproterozoic supracrustal rocks in northern Sweden. In: Bergman, S. (ed): Geology of the Northern Norrbotten ore province, northern Sweden, Rapporter och Meddelanden 141, 2018.

Hloušek, F. Malinowski, M., Bäunig, L., Buske, S., Malehmir, A., Markovic, M., Sito, L., Marsden, P., and Bäckström, E.: Three-dimensional reflection seismic imaging of the iron oxide deposits in the Ludvika mining area, Sweden, using Fresnel volume migration, Solid Earth 13, 917-934, 2022.

Hloušek, F., Jusri, T., Buske, S., Heinonen, S., Karinen, T., Kozlovskaya, E., and Leveäniemi, H.: Seismic imaging of the crustal structure in the Sodankylä region (Finland): unveling the Central Lapland Greenstone Belt's mineral potential, Geophys. J. Int. 241, 338-353, 2025.

Jensen, M.-B., Kashubin, A., Juhlin, C., and Elming, S-Å.: Multidisciplinary study of the hanging wall of the Kiirunavaara iron ore deposit, northern Sweden, Geophysics 77, B269-B285, 2012.

Juhojuntti, N., Olsson, S., Bergman, S., and Antal Lundin, I.: Reflexionsseismiska mätningar vid Kiruna – preliminär tolkning, SGU report 2014:05 (in Swedish), 2014.

Juhojuntti, N., Wood, G., Juhlin, C., O´Dowd, C., Dueck, P., and Cosma, C.: 3D seismic survey at the Millennium uranium deposit, Saskatchewan, Canada: Mapping depth to basement and imaging post-Athabasca structure near the orebody,
380   Geophysics 77, WC245-WC258, 2012.

Kennett, B.L.N.: The Seismic Wavefield. Volume I: Introduction and Theoretical Development, Cambridge University Press, 2001.

LKAB: A summary technical report on the mineral resources of LKAB, Sweden – Per Geijer Iron oxide-Apatite deposit, Available in: https://lkab.mediaflowportal.com/documents/folder/231556/, 2024.

385 Malehmir, A. and Bellefleur, G.: 3D seismic reflection imaging of volcanic-hosted massive sulfide deposits: Insights from reprocessing Halfmile Lake data, New Brunswick, Canada, Geophysics 74, B209-219, 2009.

Malmgren, L., Saiang, D., Töyrä, J., and Bodare, A.: The excavation disturbed zone (EDZ) at Kiirunavaara mine, Sweden – by seismic measurements, Journal of Applied Geophysics 61, 1-15, 2007.

Martinsson, O. and Erlandsson, M.: Prospekteringsobjekt LKAB, "Framtida järnmalmsfyndigheter i Malmfälten". Fältarbete
390   2006-2008: objekt Lappmalmen, Geovista GVR 09018, p. 68, 2009.

Pertuz, T., Malehmir, A., Brodic, B., Ding, Y., De Kunder, R., and Marsden, P.: Broadband seismic source data acquisition and processing to delineate iron-oxide deposits in the Blötberget mine - central Sweden, Geophysical Prospecting, 70, 79–94, 2021.

Smirnova, M., Juhojuntti, N., Becken, M., Smirnov, M., and the DESMEX WG: Exploring Kiruna Iron Ore fields with
395   large-scale, semi-airborne, controlled-source electromagnetics, First Break 38, 2020.

Wu, J., Milkereit, B., and Boerner, D. E: Seismic imaging of the enigmatic Sudbury Structure, Journal Geophysical Research, 100, 1995.